JOURNAL OF MATERIALS SCIENCE 19 (1984) 3732–3738

Electron probe microanalysis of nickel and chromium in Fe–C–Ni and Fe–C–Cr alloys borided at 850° C

G. PALOMBARINI
Institute of Metallurgy, University of Bologna, Italy

M. CARBUCICCHIO
Institute of Physics, University of Parma, Italy

L. CENTO
Breda Research Institute, Bari, Italy

Laboratory-cast iron–carbon alloys containing relatively low contents of nickel and chromium, respectively, were powder borided at 850° C for 4, 8 and 15 h. The redistribution of nickel and chromium between boride coatings and substrates was studied by metallography and electron probe microanalysis. It was shown that both the elements enter iron borides, substituting for iron. Chromium, however, concentrates in the coatings depleting the underlying unborided matrix, while nickel preferentially concentrates beneath the boride coatings, allowing low-Ni iron borides to be formed.

1. Introduction

In the thermochemical boriding of steels, alloying elements strongly influence total thickness, composition, structure and mechanical properties of the coatings and transition zones. The behaviour of some alloying elements, such as carbon or silicon, is well known. Owing to insolubility in iron borides, in fact, these elements diffuse into the matrix and concentrate beneath the boride layers. The carbon concentration is known to cause a reduction in total thickness and hardness of the boride layers, to change the relative stability of iron borides and to allow carbides and borocarbides to be grown in the transition zone [1–6]. Silicon, in turn, allows decarburizing processes and the formation of ferrite to be greatly enhanced in the diffusion zone, with detrimental effects on the mechanical properties of the surface layers [3–6].

On the other hand, data on the behaviour of other alloying elements, such as nickel, chromium, manganese, molybdenum, etc, appear to be contradictory. Investigating special heats of 0.45% C steel with additions of various elements, as well as industrial alloy and stainless steels borided with a powder mixture of boron carbide and boron at 950° C for 6 h, Pokhmurskii *et al.* [5] found that the maximum concentration of chromium, nickel and manganese occurred in the boride Fe_2B. From electron beam analyses of steels containing 1.05 and 1.93 wt% Mn, or 1.90 and 5.05 wt% Cr, respectively, borided by ion bombardment with diborane at temperatures as low as 600 to 700° C, Vilsmeier *et al.* [6] concluded that the solubility limits of manganese and chromium are higher in the boride Fe_2B than in the steels, but the concentration of these elements in Fe_2B is about the same as in the substrates. Using an electron microprobe technique to analyse boride layers grown at 900° C on the X20Cr13 steel, Habig and Chatterjee-Fischer [7] concluded that the chromium concentration changes very little between boride layer and base alloy. Jiang *et al.* [8], using glow discharge spectroscopy to analyse boride layers grown in 5 h at 1000° C on the Cr12Mo tool steel and 18-8 stainless steel, found that chromium concentrated in the boride layers, while nickel concentrated beneath the coatings. By a similar spectroscopic technique, Goeuriot *et al.* [9] observed an increase

0022–2461/84 $03.00 + .12

in the chromium content when crossing the interfaces from boride layers to substrates in the case of laboratory-cast binary and ternary alloys and industrial steels powder borided for 4 h at 950° C. The chromium concentration appeared to be lower in the outer FeB-base region than in the inner Fe_2B region. The opposite behaviour was displayed by nickel, which concentrated preferentially in the outer boride (FeB), causing nickel depletion of the underlying Fe_2B and subsurface layers [9].

In the present investigation, a study was made on the redistribution of chromium and nickel within the boride coatings and between coatings and substrates, after boriding Fe–C–Ni and Fe–C–Cr laboratory-cast alloys. It is well known that borides grow on pure iron giving rise to a tooth-like interface with the substrate. For columnar aggregates of borides to be obtained also on the alloys, the content of the main alloying elements was kept low (< 9 wt% Ni and < 6 wt% Cr, respectively). This columnar morphology, in fact, is particularly suitable for redistribution analyses because it is characterized by very extended coating–substrate interfaces.

The analysed boride coatings were constituted by an innermost Fe_2B single-phase layer, an intermediate region containing FeB and FeB_x with $x > 1$, and, depending on the content of the main alloying element, an outermost region containing a solid solution of iron in boron $(B, Fe)_{ss}$, in addition to FeB and FeB_x. Further details on morphology, composition, thicknesses, crystallographic textures and hardness of the boride layers have been reported previously [10, 11].

2. Experimental details

For the analysis of nickel and chromium redistribution, boride layers were grown on the ternary alloys, the composition of which is given in Table I. The alloys were laboratory-cast, homogenized by prolonged thermal treatments and borided for 4, 8 and 15 h at 850° C in contact with a B_4C-base (~ 20 wt%) powder mixture containing KBF_4 (~ 2.5 wt%) as the activator and SiC as the diluent.

TABLE I Composition of the laboratory-cast Fe–C–Me alloys

Me (wt%)	C (wt%)	Fe
Ni 2.16	0.02	balance
4.59	0.02	balance
8.85	0.02	balance
Cr 1.26	0.20	balance
2.82	0.20	balance
5.65	0.20	balance

Cross-sections of the borided samples were metallographically prepared and then analysed by means of a wavelength dispersion electron probe, with a spot ~ 3 μm in size. Concentration profiles and maps were determined for nickel and chromium, along with scanning electron micrographs of the analysed sections. Profiles were measured both normal and parallel to the external surface of the samples. The parallel profiles were taken near the layer–alloy interfaces, so as to cross both borided and untransformed regions of the substrate.

3. Results and discussion

Fig. 1 shows a metallographic cross-section of a borided Fe–C–8.85 wt% Ni alloy. On the micrograph, the lines are indicated along which the concentration profiles were measured. It is to be recalled that the innermost part of the coatings is a single-phase layer of Fe_2B, underlying an FeB-base surface layer only a few micrometres thick. Near the Fe_2B tips, and about parallel to the external surface (line a in Fig. 1), only a small redistribution of nickel can be observed: the nickel concentration appears to be lower in the Fe_2B than in the surrounding unborided matrix (Fig. 2a).

Towards the external surface (line b in Fig. 1), the nickel concentration increases appreciably in the unborided matrix around the columnar Fe_2B; correspondingly, the nickel content in the boride

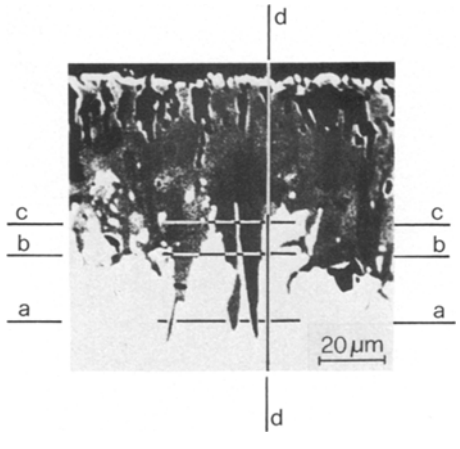

Figure 1 Metallographic cross-section of an Fe–C–8.85 wt% Ni sample borided for 15 h, showing the lines selected for nickel microanalysis.

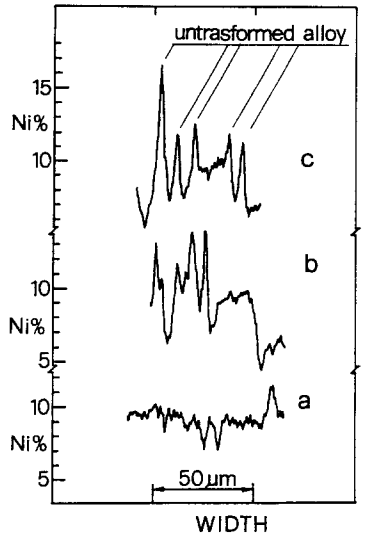

Figure 2 Nickel concentration profiles measured along lines a, b and c shown in Fig. 1.

is noticeably lower than the average value in the base alloy (Fig. 2b). The difference in the nickel concentration between Fe_2B and the surrounding matrix reaches a maximum in correspondence with the upper part of the unborided alloy (line c in Fig. 1; profile in Fig. 2c).

Fig. 3 shows a nickel concentration profile taken about normal to the external surface (line d in Fig. 1): the nickel content (i) in the unborided alloy, greatly increases just near the boride Fe_2B, and (ii) in the coating, generally remains well below the average value of that in the base alloy. In this nickel profile, fluctuations which are larger in the coating than in the base alloy should be noted. This results from the relative compactness and homogeneity of the matrix, compared to

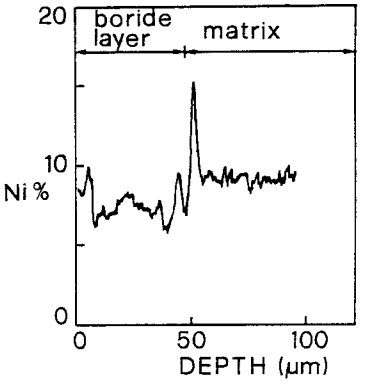

Figure 3 Nickel concentration profile measured along line d shown in Fig. 1.

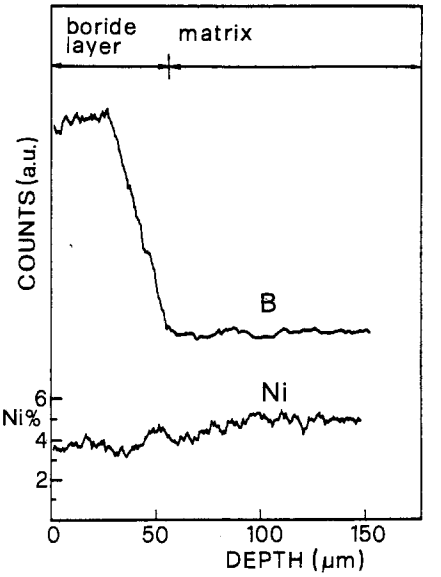

Figure 4 Boron and nickel concentration profiles, measured normal to the external surface of an Fe–C–4.59 wt% Ni sample borided for 8 h.

inhomogeneity of the coatings. In the latter, in fact:

1. different phases are present as reaction products;

2. cracks and holes formed in the outer and mechanically less-compact regions, and could be partially filled with debris coming from the base alloy during metallographic preparation;

3. zones borided in different times, and differing therefore in nickel content, coexist side by side, together with residual islands of unborided matrix.

This nickel behaviour did not change when the nickel content in the base alloy, or the length of the treatment, were changed. Fig. 4 shows boron and nickel concentration profiles measured about normal to the external surface of a 4.59 wt% Ni alloy borided for 8 h at 850° C. The mean value of nickel in the coating is appreciably lower than that measured in the matrix. At the coating–alloy interface, the boron profile reflects the coexistence of borided and unborided zones.

Figs. 5 and 6 show metallographic cross-sections of two different zones of a borided Fe–C–1.26 wt% Cr alloy. On the micrographs, the paths are indicated along which the concentration profiles were recorded. Fig. 7 shows the X-ray redistribution map for chromium corresponding to Fig. 5. Near the Fe_2B tips and parallel to the external surface (line a in Fig. 5), the

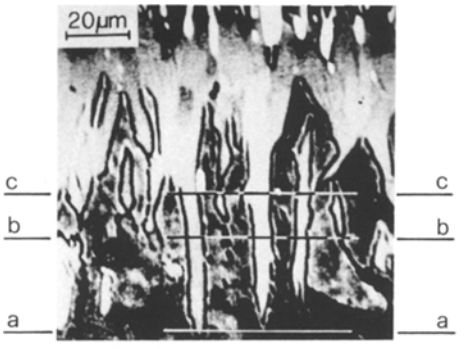

Figure 5 Metallographic cross-section of an Fe–C–1.26 wt % Cr sample borided for 15 h, showing the lines selected for chromium microanalysis parallel to the external surface.

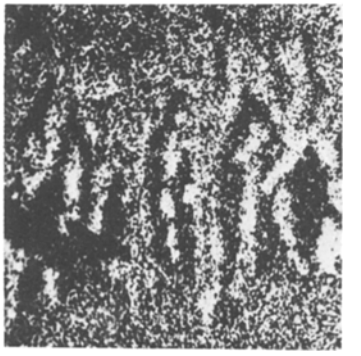

Figure 7 X-ray map for chromium, corresponding to the cross-section shown in Fig. 5.

chromium concentration undergoes no appreciable change (Fig. 8a). Going towards the external surface, concentration profiles show the tendency of chromium to concentrate within the boride Fe_2B (Figs. 8b and c), with a corresponding chromium depletion in the surrounding unborided matrix. This behaviour is opposite to that observed for nickel.

As previously observed for nickel, the peak-to-valley height differences in the chromium profile increase in going towards the external surface of the sample (Figs. 8b and c). This can be explained by the fact that the surface available for diffusion of alloying elements was increasingly large for matrix zones included between the columnar Fe_2B and towards the external surface. Moreover, the Fe_2B tips are likely to have had a lower diffusion time available.

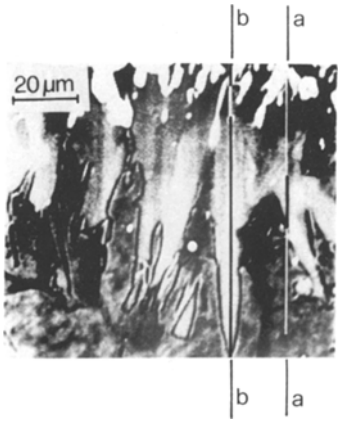

Figure 6 Another zone of the same section shown in Fig. 5, reporting the lines selected for chromium microanalysis normal to the external surface.

This conclusion is supported by the analyses carried out about normal to the external surface. Near the coating–substrate interface, in fact, the profile in Fig. 9a shows a remarkable chromium depletion within the unborided alloy, and a corresponding chromium concentration in the Fe_2B. In the profile in Fig. 9b, instead, no chromium depletion could be observed in the matrix, below the Fe_2B tips.

Local differences in structural homogeneity are likely to be responsible for the large fluctuations observed in the parts of the chromium profiles

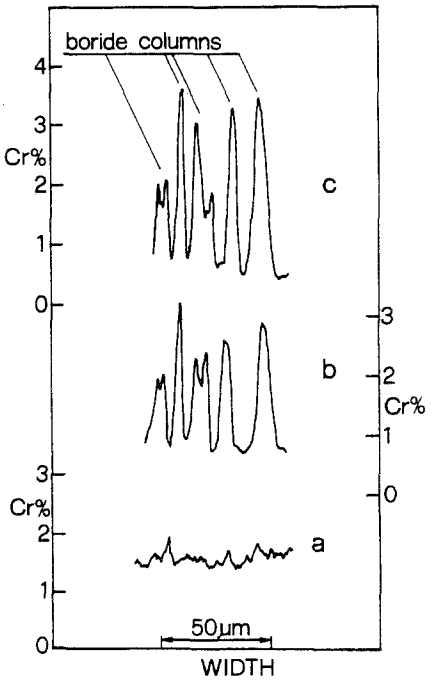

Figure 8 Chromium concentration profiles measured along lines a, b and c shown in Fig. 5.

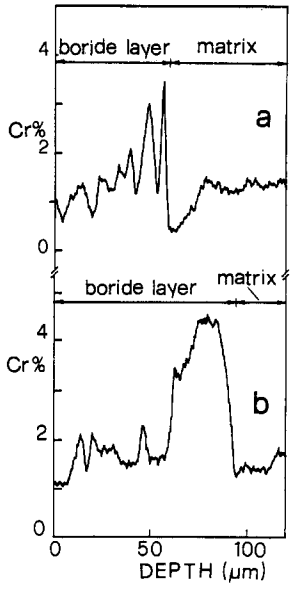

Figure 9 Chromium concentration profiles measured along lines a and b shown in Fig. 6.

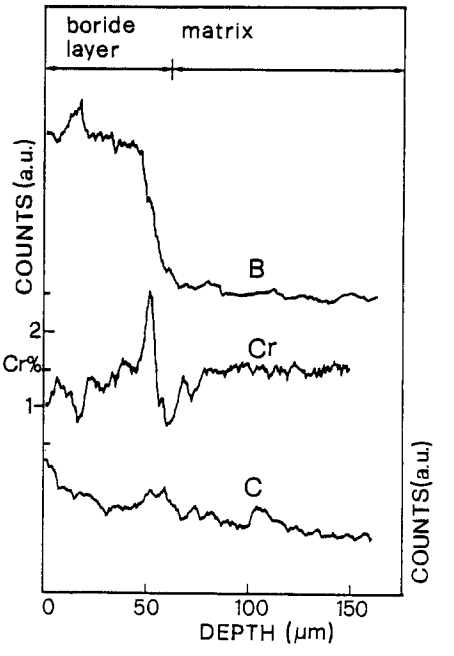

Figure 10 Nickel, boron and carbon concentration profiles measured normal to the external surface of an Fe–C–1.26 wt % Cr sample borided for 8 h.

relative to boride coatings and measured normal to the external surface (Figs. 9a and b). Sources of inhomogeneity can be the coexistence in the coatings of different phases and adjacent zones borided in successive times, as well as local failures in mechanical compactness. Considerable differences in chromium concentration in the borided chromium-containing alloys also are confirmed by chromium maps, such as that shown in Fig. 7 where, in addition to the already discussed chromium-rich columnar aggregates of boride which are surrounded by a chromium-depleted matrix, the following features are to be pointed out:

1. islands of chromium-enriched boride, mainly acicular in shape, lie in the alloy near the interface;
2. regions of unborided or recently borided matrix, which have, therefore, a relatively low chromium content, are embedded into the coating; the existence of these regions after 15 h treatment should be noted;
3. borided zones appearing compact in metallographic observation, display chromium distributions which better correspond to distinct but very closely grown aggregates.

As shown in Fig. 10, the length of treatment does not significantly change this chromium behaviour.

Fig. 11 shows a cross-section of a borided 5.65 wt % Cr ternary alloy and the paths selected to determine concentration profiles for chromium. The following differences are to be pointed out in comparison to the borided 1.26 wt % Cr alloy:

1. the columnarity of the boride layer, i.e. the difference between maximum and minimum penetration depths, is markedly lower;
2. beneath a less extended coating–substrate interface, a high density of acicular boride islands exist.

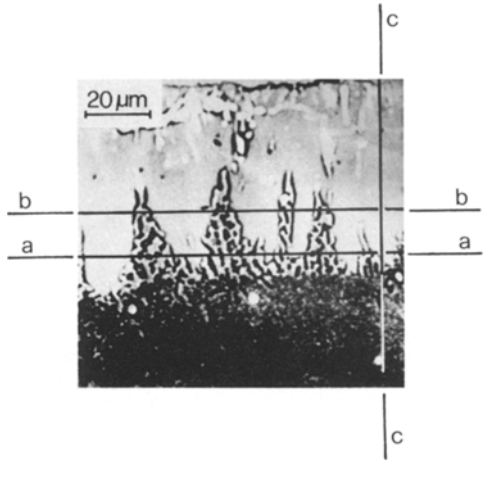

Figure 11 Metallographic cross-section of an Fe–C–5.65 wt % Cr sample, showing the lines selected for microanalysis.

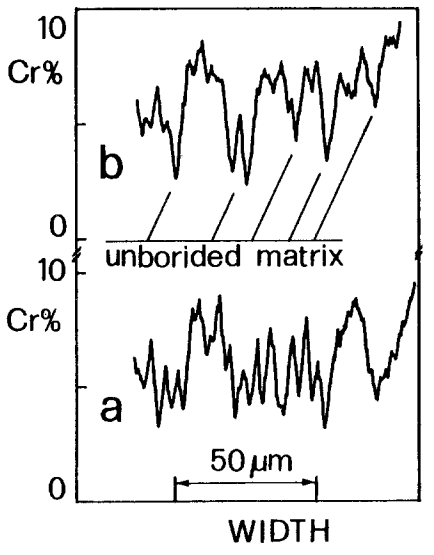

Figure 12 Chromium concentration profiles measured along lines a and b shown in Fig. 11.

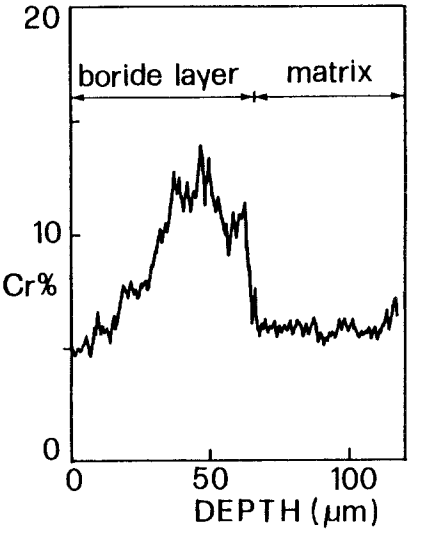

Figure 13 Chromium concentration profile measured along line c shown in Fig. 11.

The large fluctuations in the chromium concentration in the profile measured along line a in Fig. 11 and taken parallel to the external surface (Fig. 12a), can be ascribed to these particular features of the coating–substrate interface. In the profile, a remarkable increase in chromium content corresponds to the crossing of each borided area, both island and columnar aggregates, in comparison to the surrounding unborided zones.

On approaching the external surface (line b in Fig. 11), the tendency of chromium to preferentially enter iron borides depleting the neighbouring matrix appears more evident, because of higher homogeneity of the analysed adjacent zones (Fig. 12b).

The chromium profile taken about normal to the external surface (line c in Fig. 11), confirms the chromium concentration within the boride layer near the coating–alloy interface (Fig. 13). However, as already discussed for borided nickel or low-chromium containing alloys, these perpendicular profiles are strongly sensitive to the inhomogeneities which are intrinsic to the analysed coatings, and can be different depending on the path followed. Therefore, the parallel profiles allowing interfaces between differently borided compact zones to be crossed are more suitable to analyses for alloying element redistribution.

The observation that, on average, the content of chromium is higher in the coatings than in the base alloys, while the content of nickel is lower in the coatings, is in agreement with results of surface Mössbauer analyses previously carried out on the same borided alloys. Preferential entering of chromium in the coating, in fact, was able, contrary to nickel, to appreciably modify the values of the Mössbauer parameters of iron borides [10, 11].

4. Conclusions

On the basis of the analyses carried out on boride coatings thermochemically grown on ternary Fe–C–Ni and Fe–C–Cr alloys differing in the nickel and chromium contents, the following conclusions can be outlined:

1. chromium preferentially enters iron borides, causing a corresponding chromium depletion beneath the coatings. On the other hand, nickel displays a lower tendency to dissolve into borides, concentrating preferentially beneath the coatings;

2. at the interface between coating and substrate, the processes of chromium depletion and nickel concentration are particularly intense within the unborided matrix zones lying closer to the external surface. This can be ascribed to the local conditions available for diffusion of alloying elements: both surface and time for mass transfer processes, in fact, are particularly high in those zones;

3. concentration profiles measured about parallel to the external surface of the samples are more suitable to redistribution analyses of alloying elements, in that a side by side comparison is

allowed between adjacent differently boronized regions;

4. within the coatings, local inhomogeneities in the concentration of alloying elements are revealed by X-ray maps and profiles taken about normal to the external surfaces. Causes of inhomogeneity could be the coexistence of different phases (borides differing in boron content, unborided matrix, etc.), zones of the same boride formed in different times and differing, therefore, in the alloying content, as well as discontinuities in mechanical compactness;

5. on nickel-containing alloys, iron borides grow in the form of strongly columnar aggregates, despite the remarkable length of treatments and the mass transfer processes involving both the boriding species and the alloying elements, as a reasonable consequence of particularly high stress fields and lattice distortions existing in the matrix near the boride tips. On chromium-containing alloys, a columnar coating–substrate morphology only is allowed for low-chromium contents, as a consequence of preferential entering of chromium in iron borides. By increasing the chromium content in the base alloys, mass transfer phenomena and stress-field effects appear to gradually become competitive at boride–alloy interfaces, which progressively flatten.

Acknowledgements

The assistance of Dr G. Sambogna, University of Bologna, Italy, and of D. De Bartolo, Breda Research Institute, Bari, Italy, is gratefully acknowledged. This work was carried out with financial support from CNR, Italy, under "Progetto Finalizzato Metallurgia".

References

1. I. S. DUKAREVICH and M. V. MOZHAROV, Zashch. Pokrytiya Metallakh (Protective Coatings on Metals) Vol. 4, edited by G. Samsonov (Consultants Bureau, New York, 1972) p. 31.
2. V. P. SMIRNOV, A. G. BESPALOV, B. N. ZOLOTUKHIN and L. V. PAVLINOV, *ibid.*, p. 34.
3. I. S. DUKAREVICH, M. Z. MOZHAROV and A. S. SHIGAREV, *Met. Sci. Heat Treat. (USSR)* **15** (1973) 160.
4. G. WAHL, *VDI-Z.* **117** (1975) 785.
5. V. I. POKHMURSKII, V. G. PROTSIK and A. M. MOKROVA, *Sov. Mater. Sci.* **16** (1980) 185.
6. J. VILSMEIER, P. CASADESUS, Kh. G. SCHMITT-THOMAS and M. GANTOIS, *Härt.-Tech. Mitt.* **35** (1980) 24.
7. K. H. HABIG and R. CHATTERJEE-FISCHER, *Tribology Int.* **14** (1981) 209.
8. Z. S. JIANG, L. X. ZHANG, L. G. LI, X. R. PEI and T. F. LI, *J. Heat Treat.* **2** (1982) 337.
9. P. GOEURIOT, R. FILLIT, F. THEVENOT, J. H. DRIVER and H. BRUYAS, *Mater. Sci. Eng.* **5** (1982) 9.
10. M. CARBUCICCHIO, G. MEAZZA and G. PALOMBARINI, *J. Mater. Sci.* **17** (1982) 3123.
11. M. CARBUCICCHIO, E. ZECCHI, G. PALOMBARINI and G. SAMBOGNA, *ibid.* 18 (1983) 3551.

Received 16 January
and accepted 24 January 1984